Quality Evaluation of Color Demosaicing According to Image Resolution

Yanqin Yang Olivier Losson Luc Duvieubourg
Laboratoire LAGIS - CNRS UMR 8146
Université des Sciences et Technologies de Lille
Bâtiment P2 - Cité Scientifique
59655 Villeneuve d'Ascq Cedex, France
yanqin.yang@ed.univ-lille1.fr olivier.losson@univ-lille1.fr luc.duvieubourg@univ-lille1.fr

Abstract

To obtain a true color image from the Bayer CFA samples, an estimation process using interpolation is performed to retrieve the missing color components of each pixel. This is commonly referred to as CFA demosaicing. In this paper, we study the relationship between the resolution of the acquired CFA image and the quality of the demosaiced color image. For this purpose, we propose new criteria based especially on the detected edges of the objects present in the scene.

$G_{1,1}$	$R_{2,1}$	$G_{3,1}$	$R_{4,1}$	...
$B_{1,2}$	$G_{2,2}$	$B_{3,2}$	$G_{4,2}$	...
$G_{1,3}$	$R_{2,3}$	$G_{3,3}$	$R_{4,3}$	...
$B_{1,4}$	$G_{2,4}$	$B_{3,4}$	$G_{4,4}$	...
...	...	...	...	...

Figure 1. The color filter array of Bayer.

1. Introduction

Today, the majority of color cameras are equipped with a single CCD (Charge-Coupled Device) sensor. The surface of such a sensor is covered by a color filter array (CFA), which consists in a set of spectrally selective filters arranged in an alternating pattern, so that each CCD element samples only one of the three color components Red (R), Green (G) or Blue (B). The Bayer CFA is the most widely used one, it is illustrated by figure 1. To estimate the color point (R,G,B) of each pixel in a true color image, one has to determine the values of the two missing components at each pixel in the CFA image. This process is commonly referred to as CFA demosaicing, and its result as the demosaiced image.

Let us consider the case when the scene is observed simultaneously by several mono-CCD color cameras with different sizes of sensors and kinds of lenses. Therefore, the spatial resolutions (numbers of pixels) of the acquired images representing the same scene are different. The images to be processed in order to achieve a 3D reconstruction of this scene using dense stereo-matching techniques are the demosaiced ones. We need to match the homologous pixels in those images, *i.e.* pixels on which the same surface elements in the scene are projected. Such homologous pixels can be matched efficiently only if their estimated colors in the demosaiced images are close enough to each other. Consequently, the demosaicing method should be as less sensitive as possible to the resolutions of the CFA images acquired by our different cameras.

However, most of published papers (see e.g. [1], or [6] for a state of the art) have not tested the robustness of demosaicing algorithms against image resolution. In this paper, we evaluate the quality of demosaiced color images provided by several widely known methods according to image resolution (see section 2).

Since these methods intend to produce "perceptually satisfying" demosaiced images, the most widely used evaluation criteria are based on the fidelity to the original images. Rather than displaying images, our long-term goal is to match homologous pixels by means of feature analysis. These features extracted from the demosaiced images are mostly derived from either colors or detected edges. Since the quality of features is sensitive to the presence of false colors or false edges, we propose to quantify the demosaicing performance by measuring the percentages of false colors and those of false edges detected. After a brief introduction of the demosaicing methods used in our experiment, section 3 exposes the new criteria designed for low-level image analysis. In section 4, the demosaicing of images

978-0-7695-3122-9/08 $25.00 © 2008 IEEE
DOI 10.1109/SITIS.2007.33

representing the same scene with different resolutions is examined under the proposed criteria. We compare the experimental results and focus on the sensitivity of the classical demosaicing methods to image resolution.

2. Demosaicing methods introduction

Among the numerous demosaicing methods published in the literature, we present five classical methods which are tested in our experiment. They are respectively based on: bilinear interpolation [2], constant-hue interpolation [3], gradient-based interpolation [7], primary-consistent interpolation [15], and alternating projection onto convex sets [5].

2.1. Bilinear interpolation

The simplest demosaicing method uses bilinear interpolation, which estimates the missing color values at each pixel by averaging the available color components of its neighbors [2]. The estimated image exhibits two main drawbacks. One is blurring, which is caused by the smoothing effect. Furthermore, this method gives rise to false colors due to aliasing, particularly in the image areas with high spatial frequencies.

2.2. Constant-hue interpolation

To avoid those phenomena, the other methods analyze the relationships between the color components in the neighborhood to retrieve the chrominance. A common assumption is that green level represents the luminance, whereas red and blue levels correspond to the chrominance.

The constant-hue based interpolation method [3] relies on one heuristic assumption, namely that the hue of the neighbors is constant when the pixels belong to an area of the image with homogeneous colors. Here, the term "hue" refers to the ratio between chrominance and luminance, *i.e.* R/G or B/G. The red and blue values are determined so that the estimated hue changes gradually.

This method is achieved by two successive steps. First, it estimates the missing green values by bilinear interpolation. Then, it computes the missing red and blue values by weighting the green value with the average of the hues of its neighbors. This method reduces the number of false colors in homogeneous areas, but provides poor results in areas with high spatial frequencies, as can be seen from the images (a1) and (b1) of figure 7.

2.3. Gradient-based interpolation

To improve the quality of the estimated color image, the interpolation procedure should take into account whether the pixel is located in an area with homogeneous colors or is located on an edge between different objects. Moreover, when the edge is horizontal (respectively vertical), the algorithm should use the sole horizontal (resp. vertical) neighbors.

Gradient-based approaches use the horizontal and vertical gradients at a given pixel to determine the direction along which the interpolation gives the best estimation for the green component [8]. Then one can use the interpolated green values to estimate the missing red and blue by imposing, in a local neighborhood, either constant hue or equal differences between chrominances and luminances. Here we use the gradient-based interpolation method proposed by Hamilton and Adams [7], which incorprates an extra second-order correction term to estimate the green levels.

2.4. Primary-consistent interpolation

Instead of determining the interpolation direction simply by comparing the local gradients, it is necessary to use a more sophisticated measure to refine the decision. Wu and Zhang [15] explain the risk inherent in the previous gradient-based method: if the vertical and horizontal gradient at a given pixel are almost equal, the selection of the best interpolation direction should be delayed to avoid the inconsistency of the interpolation direction between the different color components. This is why the primary-consistent interpolation proposed by the authors gives better results than those provided by methods which determine directions independently for each color component.

Two candidate levels are computed to interpolate the missing green values: one is determined according to the horizontal direction, and the other according to the vertical direction. Then, the missing red and blue values are estimated both along the vertical and horizontal directions using the corresponding green candidates. Finally, the selected direction among the two tested is that along which the sum of the differences between the estimated values of $R - G$ and $B - G$ in the given area is the smallest. The candidate levels processed with this direction are retained to estimate the missing color levels of the considered pixel.

2.5. Alternating projection onto convex sets

The method proposed by Gunturk *et al.* [5] forces similar high-frequency characteristics for the R, G and B channels and ensures that the resulting image is consistent with the observed data. The two principles are enforced by defining two constraint sets, and estimating the color channels using the projections onto convex sets technique. The first set called "observation", ensures that the interpolated color is consistent with the available samples in the CFA. The second called “detail”, is based on the four subband decompositions of the color channels.

3. Measures of the demosaicing quality

Generally, the Color Mean-Square Error (CMSE) and the Color Peak Signal-to-Noise Ratio (CPSNR) [11] are used to measure the fidelity between the demosaiced image $\widehat{I}$ and the original one I. They are expressed as follows:

$$CMSE = \frac{1}{3WH} \sum_{k=R,G,B} \sum_{i=1}^{W} \sum_{j=1}^{H} (I_{i,j,k} - \widehat{I}_{i,j,k})^2 \quad (1)$$

$$CPSNR = 10 \log \left(\frac{255^2}{CMSE} \right) \quad (2)$$

where $I_{i,j,k}$ is the value of color component k of the pixel located at the spatial coordinates (i, j) in the image I, W and H are the width and height of the image in pixels, respectively.

Another measure ($\Delta E_{L^*a^*b^*}$) based on the perceptually uniform color space $CIEL^*a^*b^*$, or an extension of the latter named Spatial-CIELAB [17], is also used as a criterion in some of the papers (for example [9]). But the knowledge of the scene lighting conditions and reference white is required to use this uniform color space. As this requirement on acquisition information is seldom fulfilled for the most widely used benchmark images, the experiments have been here carried out using the CPSNR as the reference classical measure.

The CPSNR measure cannot distinguish the case when there are a high number of pixels with slight interpolation errors from the case when only a few pixels have been interpolated with severe demosaicing artifacts. However, this latter case would more significantly affect the result quality of a low-level analysis applied to the estimated image. Therefore, we propose two new criteria especially designed to determine the most effective demosaicing method for further feature extraction.

3.1. Percentage of false colors

Stereo-matching algorithms based on a color correlation measure are very sensitive to false colors. At a given pixel in the original and demosaiced images, any mere change of one color component level can be considered as false color. In reality, we have to take into account that the human vision system cannot distinguish such subtle difference below a certain level [4]. Therefore, we consider that the estimated color $\widehat{I}_{i,j}$ at a given pixel $P_{i,j}$ is false if it differs from the original color $I_{i,j}$ by at least a threshold value T for one among its three color components. We define the percentage of false colors, denoted $FC_{\%}$, as the ratio of the number of pixels detected with false colors to the image size $W \times H$:

$$FC_{\%} = \frac{100}{WH} \operatorname{card} \left\{ P_{i,j} \mid \max_{k=R,G,B} \left(\left| I_{i,j,k} - \widehat{I}_{i,j,k} \right| \right) > T \right\} . \quad (3)$$

3.2. Percentage of false edges detected

Artifacts generated by demosaicing (mostly blurring and false colors) may affect the performance of edge detection methods applied to the demosaiced image. Indeed, blurring reduces the sharpness of edges, and false colors can give rise to irrelevant edges. That is why we propose to quantify the effect of the demosaicing methods on edge detection performance.

We threshold the module of the vector gradient proposed by Di Zenzo [16] with identical parameters to detect edges both in the original I and the demosaiced $\widehat{I}$ images and obtain two binary edge images B and $\widehat{B}$. To measure the effects of artifacts on the detected edge locations, we compare the two edge images by examining the sub-detected edges and the over-detected edges. [14]

As shown on figure 2, the binary image SD contains sub-detected edges, namely edge pixels detected in the original image I and not retrieved in the demosaiced one $\widehat{I}$. Respectively the binary image OD contains over-detected edges, namely erroneously detected edge pixels in the demosaiced image $\widehat{I}$. For quantifying these observations, we propose to compute the sub-detected $SD_{\%}$ and over-detected $OD_{\%}$ edge pixel percentages, respectively defined as:

$$SD_{\%} = \frac{\operatorname{card}\{P_{i,j} \mid SD_{i,j} \neq 0\}}{\operatorname{card}\{P_{i,j} \mid B_{i,j} \neq 0\}} \text{ , and} \quad (4)$$

$$OD_{\%} = \frac{\operatorname{card}\{P_{i,j} \mid OD_{i,j} \neq 0\}}{\operatorname{card}\{P_{i,j} \mid \widehat{B}_{i,j} \neq 0\}} . \quad (5)$$

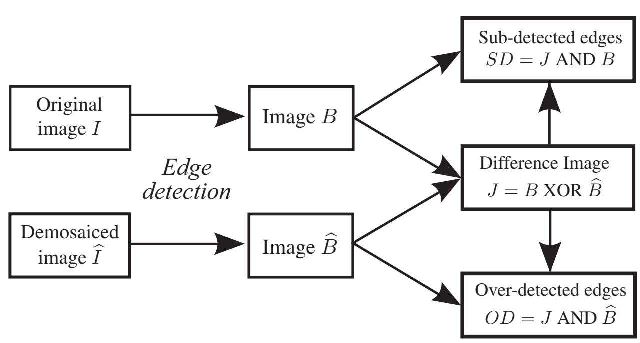

Figure 2. Sub- and over-detection of edges.

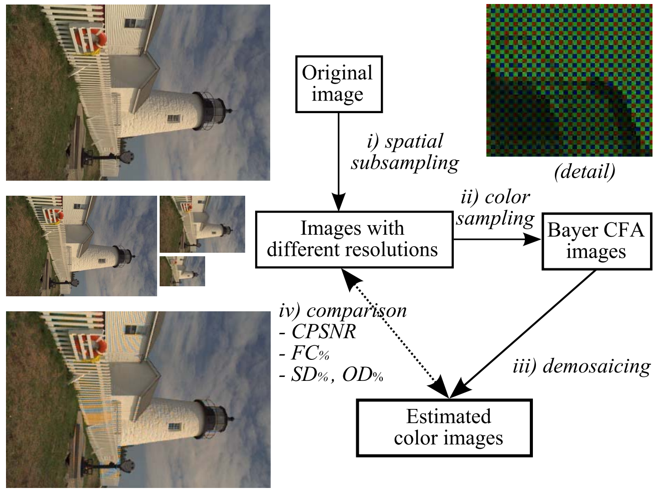

Figure 3. Global procedure used for demosaicing quality evaluation (example of image "*Lighthouse*").

4. Experimental results

4.1. Description of the procedure

The experimental procedure (see figure 3) is decomposed into four successive steps:

1 sub-sample the original color image to simulate the acquisition of the images with different spatial resolutions as mentioned in [15] and [13]. The original size of the image being 768×512 ($W \times H$), the zoomed image of size 384×256 is obtained by averaging every juxtaposed 2×2 pixel blocks on each of the three color components. Other image resolutions are obtained by increasing the block size (here we consider only images with reduced resolution);

2 simulate the color sampling by keeping only one out of three color components at every pixel, according to the spatial arrangement of the Bayer CFA of figure 1;

3 apply the local interpolation methods described above to obtain true color images from the CFA ones (this is the demosaicing step);

4 measure the demosaicing quality by comparing the original I and estimated $\widehat{I}$ images with the same resolution.

4.2. Demosaicing quality results

4.2.1 CPSNR

We have carried out the experiment by measuring the CPSNR provided by the five interpolation methods mentioned in section 2, applied to 12 images of the Kodak database [12] (see figure 4).

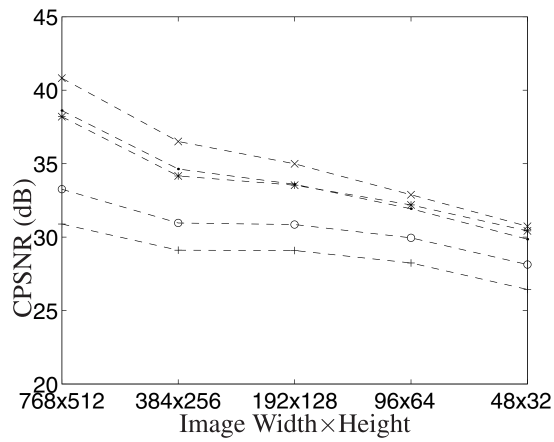

Figure 4. CPSNR values for different resolutions (averages over the 12 images). Interpolation methods: bilinear ($+$), constant-hue based ($\circ$), gradient-based ($*$), primary-consistent ($\cdot$), alternating projection ($\times$).

It can be noticed that, for all the methods, the fidelity level falls when the resolution decreases. This figure proves that the available demosaicing methods are quite sensitive to image resolution, which corroborates the results stated in [13].

Moreover, the relative performance reached by the five methods is preserved over all spatial resolutions: the bilinear and constant-hue based interpolations produce the lowest CPSNR values, while the algorithm using the alternating

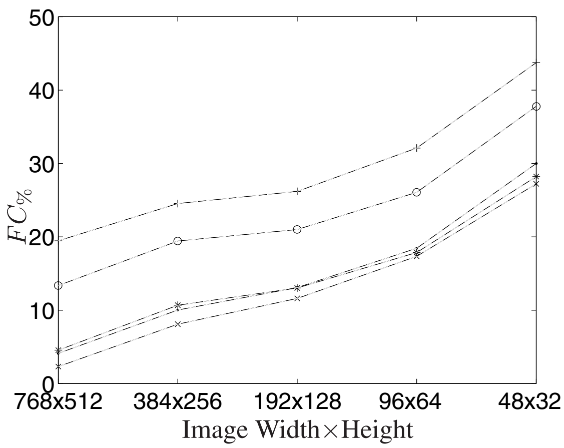

Figure 5. Percentage of pixels estimated with false colors, for different resolutions (averages over the 12 images). The legend is the same as in figure 4.

projection onto convex sets always performs best.

4.2.2 Percentage of false colors

Plots of figure 5 illustrate the influence of image resolution on the percentage of false colors. One can notice that the relative performance among the methods is again largely independent upon the resolution: the alternating projection method always performs best in terms of pixels estimated with false colors. Likewise, the primary-consistent and gradient-based algorithms supply good results, while requiring far less computation time.

In addition, those results are consistent with the ones obtained by using the CPSNR. The demosaicing algorithms which yield the fewest pixels with false colors correspond to those leading to the highest CPSNR scores. Moreover, the evolution of the percentage of false colors is again monotonous according to the image resolution, whatever the demosaicing method considered.

4.2.3 Percentage of false edges detected

Figure 6 illustrates the percentages of sub-detected (a) and over-detected (b) edge pixels according to the resolution. By examining these plots, we notice that the computed percentages increase significantly when the resolution is reduced. In addition, the performance order of the demosaicing methods is globally preserved through all resolutions. Once again, the alternating projection method yields the best results, as for the two previous criteria.

The edge detection procedure is sensitive to both types of demosaicing artifacts. Low-pass filtering tends to smooth edges, while false colors or the so-called *zipper effect* (an alternate on-off pattern with repeated and unnatural colors) may give rise to abnormally high values of Di Zenzo gradient module. The respective expected consequences are sub- and over-detection of edges. One can notice that the different demosaicing algorithms are more or less efficient in avoiding to generate either blurring or false color artifacts.

The study of the edge detection quality (illustrated in figure 6) alone does not allow to conclude which kind of artifact is predominant in the various interpolation methods. Indeed, the ratios of sub-detected and over-detected edge pixels are globally comparable in pairs, for a given method and a given resolution. Nevertheless, unlike CPSNR, a low-level local analysis (such as the color edge detection) enlightens the image areas where colors have been badly estimated or smoothed by demosaicing (see figure 6(c), and figure 7 for visual details). This is a key point to evaluate the demosaicing algorithms in regard to the results of feature detection procedures. Taking a close look at the figure 7, we can find that the errors of the edge detection predominantly occur in the areas with high spatial frequency.

5 Conclusion

This paper lies within the context of stereo-matching of images with different resolutions acquired by mono-CCD cameras. Such procedures are based on extracted features, which are sensitive to both resolution and color demosaicing. Therefore, we study the relationship between resolution and demosaicing quality, and propose new criteria designed for low-level image analysis.

Experimental results show that low-level features (colors or edges) extracted from demosaiced images are affected by resolution, whatever the demosaicing method used. It would be interesting to extend these experiments by evaluating the quality of stereo-matching against image resolution.Moreover, the alternating projection algorithm provides the best results among the demosaicing methods under consideration here.

In the above experiments, the reduction of image resolution was simply achieved by averaging the pixel color levels over juxtaposed blocks. Actually, one should consider a more sophisticated image formation model to simulate better what happens in a real camera. Complex models have been proposed for CCD color cameras [10], which can be satisfyingly approximated by the Point Spread Function (PSF) of the lens and by taking into account the noise of the electronic device. We started to use a Gaussian Filter to represent the PSF and assumed the overall noise was Gaussian distributed. This has lead to more realistic low-resolution images, which should now be incorporated in our study.

Another work in progress is to examine the correlation between the demosaicing artifacts and edge detection, in

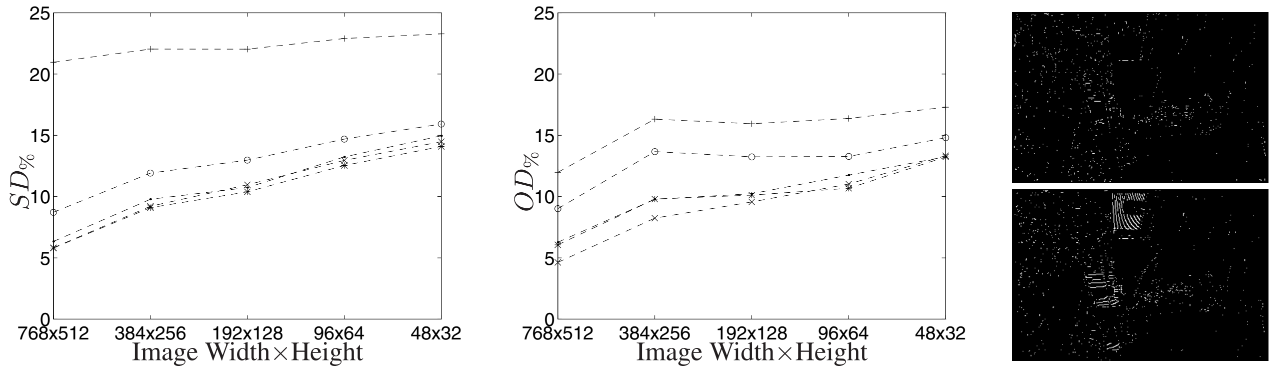

(a) (b) (c)

Figure 6. Percentages of sub-detected (a) and over-detected (b) edges, for different resolutions (averages over the 12 images and same legend as in figure 4). Subfigure (c) shows the corresponding SD (up) and OD (down) results for the image used in figure 3, with resolution 384×256.

order to develop a demosaicing method which does not decrease the edge detection quality when the image resolution is reduced.

6 Acknowledgements

The authors thank the Nord-Pas-de-Calais Regional Council and the UE for the grant FEDER N.4OBJ2-2005/3-4.1-253PRESAGE-7820.

References

[1] D. Alleysson, S. Süsstrunk, and J. Hérault. Linear demosaicing inspired by the human visual system. *IEEE Transactions on Image Processing*, 14(4):439–449, Apr. 2005.

[2] D. Cok. Single-chip electronic color camera with color-dependent birefringent optical spatial frequency filter and red and blue signal interpolating circuit. US patent 4,605,956, to Eastman Kodak Co., Patent and Trademark Office, Washington D.C., 1986.

[3] D. R. Cok. Reconstruction of CCD images using template matching. In *Procs. of the IS&T's 47th Annual Conference, Physics and Chemistry of Imaging Systems (ICPS'94)*, volume 2, pages 380–385, Rochester,NY,USA, May 1994.

[4] O. Faugeras. Digital color image processing within the framework of a human visual model. *IEEE Transactions on Acoustics, Speech, and Signal Processing*, 27(4):380–393, Aug. 1979.

[5] B. K. Gunturk, Y. Altunbasak, and R. M. Mersereau. Color plane interpolation using alternating projections. *IEEE Transactions on Image Processing*, 11(9):997–1013, Sept. 2002.

[6] B. K. Gunturk, J. Glotzbach, Y. Altunbasak, R. W. Schafer, and R. M. Mersereau. Demosaicking : Color filter array interpolation. *IEEE Signal Processing Magazine*, 22(1):44–54, Jan. 2005.

[7] J. Hamilton and J. Adams. Adaptive color plan interpolation in single sensor color electronic camera. US patent 5,629,734, to Eastman Kodak Co., Patent and Trademark Office, Washington D.C., 1997.

[8] R. Hibbard. Apparatus and method for adaptively interpolating a full color image utilizing luminance. US patent 5,382,976, to Eastman Kodak Co., Patent and Trademark Office, Washington D.C., 1995.

[9] K. Hirakawa and T. W. Parks. Adaptive homogeneity-directed demosaicing algorithm. *IEEE Transactions on Image Processing*, 14(3):360–369, Mar. 2005.

[10] V. Krasnjuk, D. Arandjeklovic, M. Petrovic, and M. Hribsek. A CCD model applied to colour camera characteristics measurement. In *Procs. International Broadcasting Convention (IBC'94)*, pages 411–414, Amsterdam, The Netherlands, Sept. 1994.

[11] H. Li, L. Chang, and Y.-P. Tan. Performance factors for evaluating color filter array demosaicking algorithms. In *Procs. IEEE International Conference on Information, Communications and Signal Processing (ICICS 2005)*, pages 1302–1306, Bangkok, Thailand, Dec. 2005.

[12] X. Li. http://www.csee.wvu.edu/xinl/demo/demosaic.html.

[13] W. Lu and Y.-P. Tan. Color filter array demosaicking: New method and performance measures. *IEEE Transactions on Image Processing*, 12(10):1194–1210, Oct. 2003.

[14] D. Martin, C. Fowlkes, and J. Malik. Learning to detect natural image boundaries using local brightness, color, and texture cues. *IEEE Transactions on Pattern Analysis and Machine Intelligence*, 26(5):530–549, May 2004.

[15] X. Wu and N. Zhang. Primary-consistent soft-decision color demosaicking for digital cameras. *IEEE Transactions on Image Processing*, 13(9):1263–1274, Sep. 2004.

[16] S. D. Zenzo. A note on the gradient of a multi-image. *Computer Vision, Graphics, and Image Processing*, 33(1):116–125, Jan. 1986.

[17] X. Zhang and B. Wandell. A spatial extension of CIELAB for digital color reproduction. In *Procs. Society for Information Display Symposium Technical Digest*, volume 27, pages 731–734, San Diego,CA,USA, Feb. 1996.

(a_1)

(a_2)

(b_1)

(b_2)

Figure 7. Estimated image (up) and difference image (down) $J = B \ \mathrm{OR} \ \widehat{B}$ of detected edges, with two different resolutions: (a) $768{\times}512$ and (b) $384{\times}256$ (zoomed in by a factor 2 for illustration purpose), obtained by two demosaicing methods : constant-hue based (subscript 1) and alternating projection (subscript 2).